INTERNATIONAL JOURNAL FOR NUMERICAL METHODS IN FLUIDS
Int. J. Numer. Meth. Fluids 2004; **46**:485–505 (DOI: 10.1002/fld.767)

Accuracy analysis of super compact scheme in non-uniform grid with application to parabolized stability equations

V. Esfahanian[1,*,†], S. Ghader[2] and Kh. Ashrafi[2]

[1]*Department of Mechanical Engineering, University of Tehran, Iran*
[2]*Atmospheric Science & Meteorological Research Center, Iran*

SUMMARY

A brief derivation of the super compact finite difference method (SCFDM) in non-uniform grid points is presented. To investigate the accuracy of the SCFDM in non-uniform grid points the Fourier analysis is performed. The Fourier analysis shows that the grid aspect ratio plays a crucial role in the accuracy of the SCFDM in a non-uniform grid. It is also found that the accuracy of the higher order relations of the SCFDM is more sensitive to grid aspect ratio than the lower order relations. In addition, to obtain a mathematical representation of the accuracy and making clear the role of the aspect ratio in the accuracy of the SCFDM in non-uniform grids, the modified equation approach is used. For the sake of demonstrating the analytical results obtained from the Fourier analysis and the modified equation approach, the super compact finite difference method is applied to solve the Blasius boundary layer and the non-linear parabolized stability equations as numerical examples indicating the difficulty with non-uniform grid spacing using the super compact scheme. Copyright © 2004 John Wiley & Sons, Ltd.

KEY WORDS: super compact scheme; numerical accuracy; non-uniform grid; Fourier analysis; modified equation; Blasius boundary layer; PSE

1. INTRODUCTION

High-order compact finite difference methods have been the subject of numerous papers in which they have been successfully applied to the problems in fluid dynamics. Historically these methods may be traced back to Numerov [1] and Fox and Goodwin's [2] work. But it was the suggestion of Kreiss [3] and Hirsh's paper [4] that made these methods an important tool for accurate simulation of the fluid dynamic problems. Many classes of the compact schemes have been derived in recent years. For example, Lele [5] analysed compact finite difference methods with spectral-like resolutions and also studied the accuracy of these schemes.

*Correspondence to: V. Esfahanian, Department of Mechanical Engineering, University of Tehran, Campus No. 2, North Karegar Avenue, Tehran, Iran.
†E-mail: evahid@ut.ac.ir

Contract/grant sponsor: University of Tehran
Contract/grant sponsor: Atmospheric Science & Meteorological Research Center (ASMERC) of Iran

Published online 18 August 2004

Received 5 May 2003
Revised 22 January 2004

A general class of highly accurate finite difference schemes called super compact finite difference method (SCFDM) has been introduced by Dexun Fu and Yanwen Ma [6]. The formulation of this method and its derivation in non-uniform and uniform grids have been presented in References [6, 7] and Reference [8], respectively. In addition, the application of the method in uniform grid has been studied in Reference [9].

In many numerical studies of fluid flow where sever gradients are to be expected i.e. in boundary layer, non-uniform grids are required to obtain an accurate solution. The objective of the present work is to investigate the accuracy of the super compact finite difference method in non-uniform grid points.

To address the issue, Section 2 represents a brief derivation of the SCFDM in non-uniform grid points. In Section 3, the accuracy of the method is investigated using the Fourier analysis. The modified equation approach is discussed in Section 4. The solution of the Blasius boundary layer and non-linear parabolized stability equations using SCFDM in non-uniform grid points are presented in Sections 5 and 6 as numerical examples. Finally, Section 7 gives the main conclusions.

2. DERIVATION OF THE SCFDM IN NON-UNIFORM GRID

The SCFDM has two general equations namely, basic equation and auxiliary equations. These equations are obtained by using the Taylor series. A forward discrete Taylor series for an arbitrary function, f, in any direction, x, and in a non-uniform grid can be written as:

$$f_{j+1} = f_j + h_j f'_j + \frac{h_j^2}{2!} f''_j + \cdots \tag{1}$$

where $h_j = x_{j+1} - x_j$. By defining a forward operator as

$$\delta_x^+ f_j = f_{j+1} - f_j$$

Equation (1) can be rewritten as follows:

$$\delta_x^+ f_j = h_j f'_j + \frac{h_j^2}{2!} f''_j + \cdots \tag{2}$$

Using the same procedure a similar equation for backward Taylor series can be obtained,

$$\delta_x^- f_j = h_{j-1} f'_j - \frac{h_{j-1}^2}{2!} f''_j + \cdots \tag{3}$$

where $\delta_x^- f_j = f_j - f_{j-1}$ and $h_{j-1} = x_j - x_{j-1}$. The basic equation of the SCFDM is achieved by adding Equations (2) and (3) as below:

$$(\alpha\delta_x^+ + \beta\delta_x^-) f_j = \frac{1}{1!}[\alpha + \beta\sigma_j] f_j^{\langle 1\rangle} + \frac{1}{2!}[\alpha - \beta\sigma_j^2] f_j^{\langle 2\rangle} + \cdots$$

$$+ \frac{1}{n!}[\alpha + (-1)^{n+1}\beta\sigma_j^n] f_j^{\langle n\rangle} \tag{4}$$

where

$$\sigma_j = \frac{h_{j-1}}{h_j}, \quad f_j^{\langle k \rangle} = h_j^k \left(\frac{\partial^k f}{\partial x^k} \right)_j$$

in which α and β are free parameters. It can be seen that the basic equation relates function f to the higher derivatives. In this equation the number of unknowns are much more than equations thus some additional equations namely, the auxiliary equations are needed to close the system. The auxiliary equations are obtained similar to the basic equation i.e. for each derivative of f (e.g. lth derivative) the forward and backward discrete Taylor series are written and then are added. Then by using the previous definitions, auxiliary equations can be obtained as follows:

$$\sigma_{j+1}^l f_{j+1}^{\langle l \rangle} - 2 f_j^{\langle l \rangle} + \frac{1}{\sigma_j^l} f_{j-1}^{\langle l \rangle} = \frac{1}{1!}(1-\sigma_j) f_j^{\langle l+1 \rangle} + \frac{1}{2!}(1+\sigma_j^2) f_j^{\langle l+2 \rangle} + \cdots + \frac{1}{(n-l)!}(1+(-1)^{n-l}\sigma_j^{n-l}) f_j^{\langle n \rangle} \tag{5}$$

Introducing the vectors

$$\mathbf{F} = \{f^{\langle 1 \rangle}, f^{\langle 2 \rangle}, \ldots, f^{\langle n \rangle}\}^{\mathrm{T}}, \quad \mathbf{E} = \{1, 0, \ldots, 0\}^{\mathrm{T}}$$

and the matrices

$$\mathbf{A} = \frac{1}{2} \begin{pmatrix} \dfrac{\alpha+\beta\sigma}{1!} & \dfrac{\alpha-\beta\sigma^2}{2!} & \cdots & \dfrac{\alpha+(-1)^{n+1}\beta\sigma^n}{n!} \\ 0 & \dfrac{1-\sigma}{1!} & \cdots & \dfrac{1+(-1)^{n-1}\sigma^{n-1}}{(n-1)!} \\ 0 & 0 & \cdots & \dfrac{1+(-1)^{n-2}\sigma^{n-2}}{(n-2)!} \\ \cdots & \cdots & \cdots & \cdots \\ 0 & 0 & \cdots & \dfrac{1-\sigma}{1!} \end{pmatrix}$$

$$\mathbf{L} = \begin{pmatrix} 0 & 0 & 0 & 0 & \cdots & 0 \\ \sigma & 0 & 0 & 0 & \cdots & 0 \\ 0 & \sigma^2 & 0 & 0 & \cdots & 0 \\ 0 & 0 & \sigma^3 & 0 & \cdots & 0 \\ \cdots & \cdots & \cdots & \cdots & \cdots & \cdots \\ 0 & 0 & 0 & \cdots & \sigma^{n-1} & 0 \end{pmatrix}$$

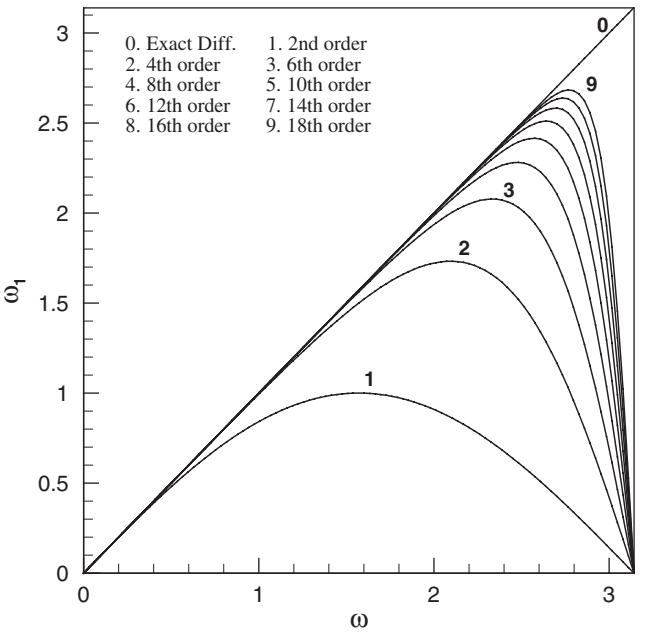

Figure 1. Variations of the modified wave number for the first derivative approximation for the SCFDM with $\sigma_j = 1$.

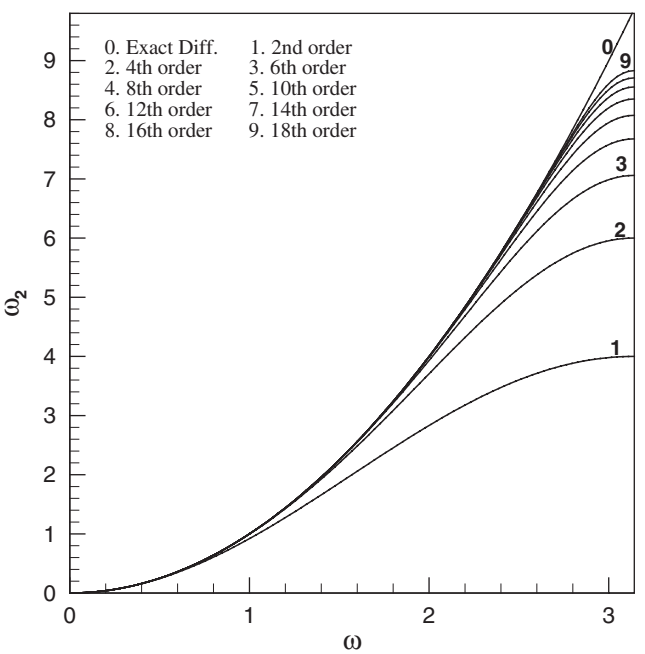

Figure 2. Variations of the modified wave number for the second derivative approximation for the SCFDM with $\sigma_j = 1$.

Equations (4) and (5) can be rewritten into a vector form and the following relation is obtained:

$$-\frac{1}{2}\mathbf{L}\left(\frac{1}{\sigma_j}\right)\mathbf{F}_{j-1}+(\mathbf{A}+\mathbf{L})\mathbf{F}_j-\frac{1}{2}\mathbf{L}(\sigma_{j+1})\mathbf{F}_{j+1}=\frac{1}{2}(\alpha\delta_x^+ +\beta\delta_x^-)f_j\mathbf{E} \tag{6}$$

$\mathbf{L}$ and $\mathbf{A}$ are $N\times N$ matrices, $\mathbf{F}$ and $\mathbf{E}$ are N dimensional vectors and $f_j^{\langle k\rangle}/h_j^k$ approximates $\partial^k f/\partial x^k$ with the accuracy of order $N-k+1$. In the case $\sigma_j=1$, the coefficients in relation (6) do not depend on the co-ordinate direction and the mesh grid points. At the boundaries, forward and backward relations are used. These relations are derived similar to central relations [8].

By choosing $\alpha=\beta=1$, $\sigma_j=1$ and $\alpha=-\beta=1$, $\sigma_j=1$ the SCFDM relations for odd and even derivatives can be obtained in a uniform grid, respectively. For these relations the plots of the modified wave numbers for the first and the second derivatives approximation of the SCFDM using the Fourier analysis are given in Figures 1 and 2.

3. ACCURACY ANALYSIS

In this section, the Fourier analysis is used to investigate the accuracy of the SCFDM in non-uniform grid points. A single Fourier mode,

$$f_j=\exp(\mathrm{i}\omega s),\quad s=\frac{x_j}{h_j},\quad \mathrm{i}=\sqrt{-1} \tag{7}$$

is chosen for the Fourier analysis [5, 10]. As an example, the Fourier analysis is applied to SCFDM relations by setting $N=3$, in this case Equations (4) and (5) can be written as follows:

$$\begin{gathered}(\alpha\delta_x^+ +\beta\delta_x^-)f_j=(\alpha+\beta\sigma_j)h_jf_j'+\tfrac{1}{2}(\alpha-\beta\sigma_j^2)h_j^2f_j''+\tfrac{1}{6}(\alpha+\beta\sigma_j^3)h_j^3f_j'''\\ h_jf_{j+1}'-2h_jf_j'+h_jf_{j-1}'=(1-\sigma_j)h_j^2f_j''+\tfrac{1}{2}(1+\sigma_j^2)h_j^3f_j'''\\ h_j^2f_{j+1}''-2h_j^2f_j''+h_j^2f_{j-1}''=(1-\sigma_j)h_j^3f_j'''\end{gathered} \tag{8}$$

By substituting Equation (7) into Equation (8) a complex system of equations is obtained. By decomposing this complex system to the real and imaginary parts, a system of equations for the modified wave numbers can be obtained as follows:

$$\begin{gathered}(\alpha+\beta)\sin\omega=(\alpha+\beta\sigma_j)\omega_1-\tfrac{1}{6}(\alpha+\beta\sigma_j^3)\omega_3\\ (\alpha-\beta)(1-\cos\omega)=\tfrac{1}{2}(\alpha-\beta\sigma_j^2)\omega_2\\ 2\omega_1(1-\cos\omega)=\tfrac{1}{2}(1+\sigma_j^2)\omega_3\end{gathered} \tag{9}$$

where ω_1, ω_2 and ω_3 are modified wave numbers of the first, second and third derivatives, respectively. By solving the system of equations (9), the modified wave numbers ω_1 and ω_2

(ω_3 is not presented here) are obtained as:

$$\omega_1 = \frac{3(1+\sigma_j^2)(\alpha+\beta)\sin\omega}{3(1+\sigma_j^2)(\alpha+\beta\sigma_j) - 2(1-\cos\omega)(\alpha+\beta\sigma_j^3)}$$
$$\omega_2 = \frac{2(\alpha-\beta)(1-\cos\omega)}{(\alpha-\beta\sigma_j^2)} \tag{10}$$

It is obvious that ω_1, ω_2 and ω_3 are found implicitly. From Equation (10) it can be easily seen that the modified wave numbers ω_1 and ω_2 do not depend on the parameters α and β, in uniform grid points ($\sigma_j = 1$). This is a general property of the SCFDM. The effect of α and β is investigated in the following section.

3.1. Accuracy analysis of the sixth-order formulation

In this section, the effects of aspect ratio, $k = 1/\sigma_j$, and free parameters α and β, on the accuracy of the sixth-order SCFDM relations are investigated. As it was mentioned before, the modified wave numbers are obtained implicitly. The plots of the modified wave numbers ω_1 and ω_2 for several aspect ratios ($\alpha = 1$, $\beta = \pm 1$) are presented in Figures 3 and 4. It can be seen from these figures that the accuracy begins to change when the aspect ratio k increases. For k close to one, the accuracy behaves almost like uniform grid. But when k is far away from one, the accuracy decreases and the method is not as accurate as it was expected.

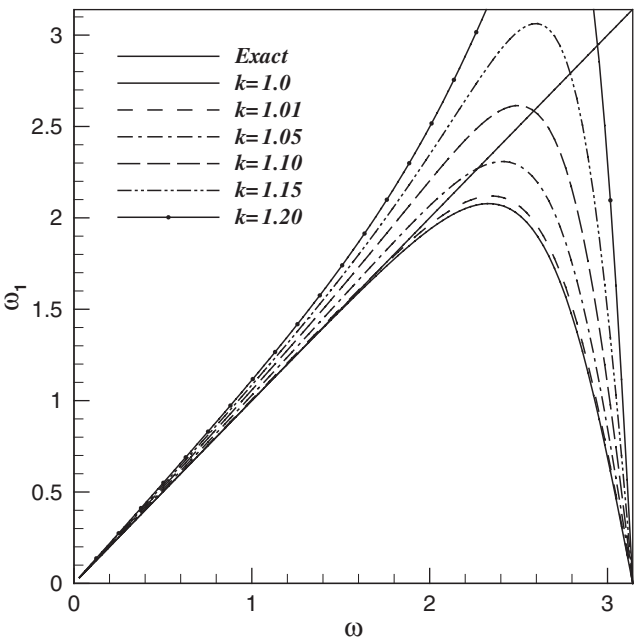

Figure 3. Comparisons of the first modified wave number for different values of k ($\alpha = 1$ and $\beta = 1$).

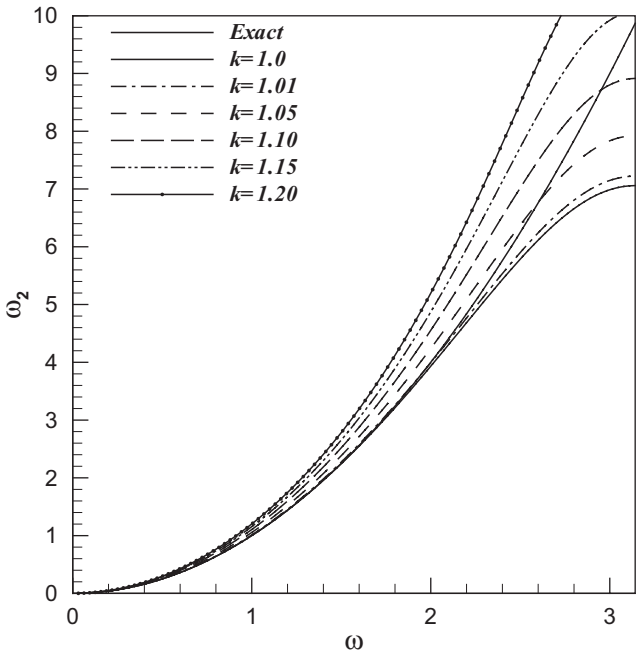

Figure 4. Comparisons of the second modified wave number for different values of k ($\alpha = 1$ and $\beta = -1$).

To investigate the effect of parameters α and β, the plots of the modified wave numbers ω_1 and ω_2 are presented in two cases. Figures 5 and 6 show these plots for the case $k = 1.1$. The results for the case $k = 1.01$ are shown in Figures 7 and 8. It can be seen from these figures that by choosing suitable parameters α and β, the accuracy can be improved. Figures 9 and 10 show the effect of decreasing the aspect ratio on the accuracy.

Similar investigation is performed for the eighth-order SCFDM. The plots of the modified wave numbers ω_1 and ω_2 for several aspect ratios ($\alpha = 1$, $\beta = \pm 1$) are presented in Figures 11 and 12. It can be seen from these figures that the eighth-order SCFDM relations are more sensitive to the grid aspect ratio respect to the sixth-order relations.

Here, it is interesting to compare the accuracy of the sixth-order super compact method with the sixth-order traditional method. The sixth-order accurate traditional finite difference method is expressed as (e.g. Reference [9])

$$f_j^{\langle 1 \rangle} = \tfrac{1}{60}[45(f_{j+1} - f_{j-1}) - 9(f_{j+2} - f_{j-2}) + (f_{j+3} - f_{j-3})] \tag{11}$$

The Fourier analysis of Equation (11) in uniform grid leads to the following modified wave number

$$\omega_1 = \frac{45\sin(\omega) - 9\sin(2\omega) + \sin(3\omega)}{30} \tag{12}$$

After the derivation of the sixth-order accurate traditional finite difference method in a non-uniform grid and by using the Fourier analysis, the corresponding modified wave number will

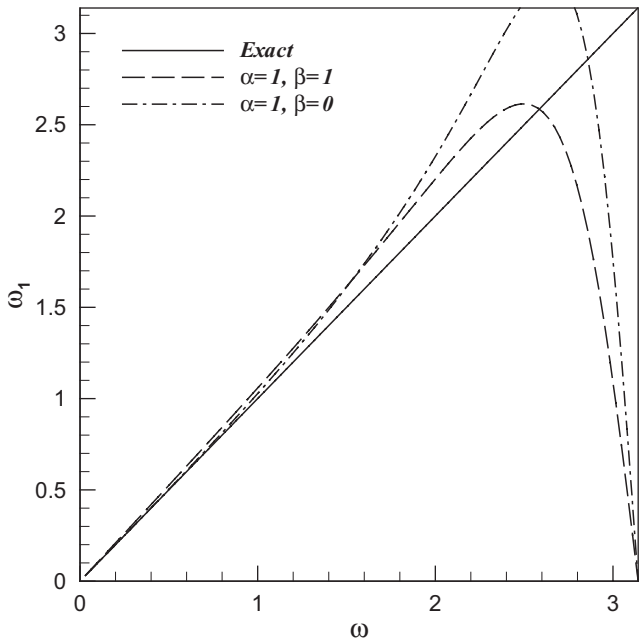

Figure 5. Comparisons of the first modified wave number for $k = 1.1$ and two different values $\alpha = 1, \beta = 1$ and $\alpha = 1, \beta = 0$.

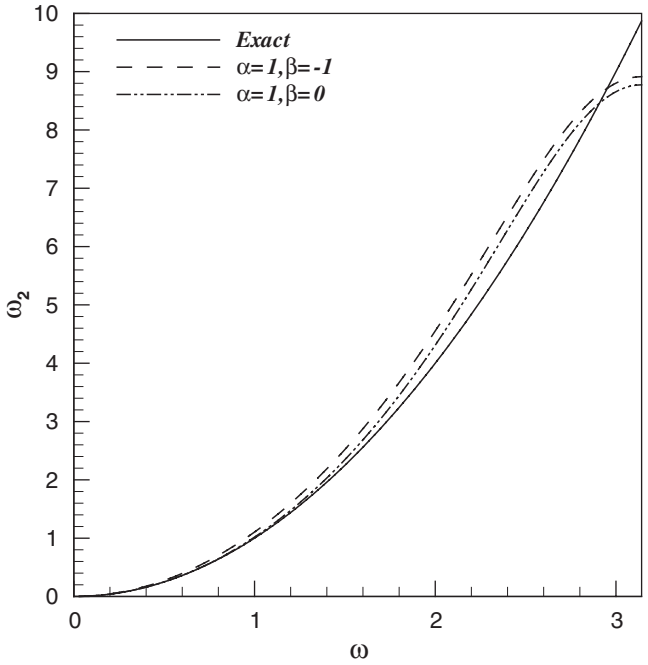

Figure 6. Comparisons of the second modified wave number for $k = 1.1$ and two different values $\alpha = 1, \beta = -1$ and $\alpha = 1, \beta = 0$.

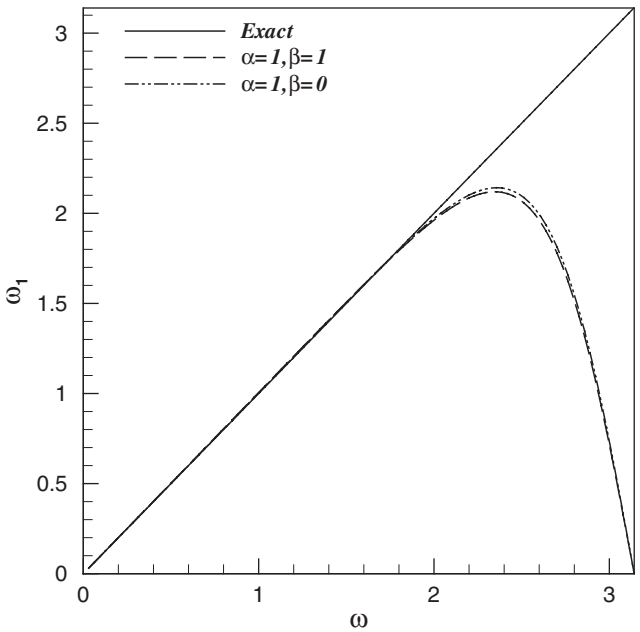

Figure 7. Comparisons of the first modified wave number for $k = 1.01$ and two different values $\alpha = 1, \beta = 1$ and $\alpha = 1, \beta = 0$.

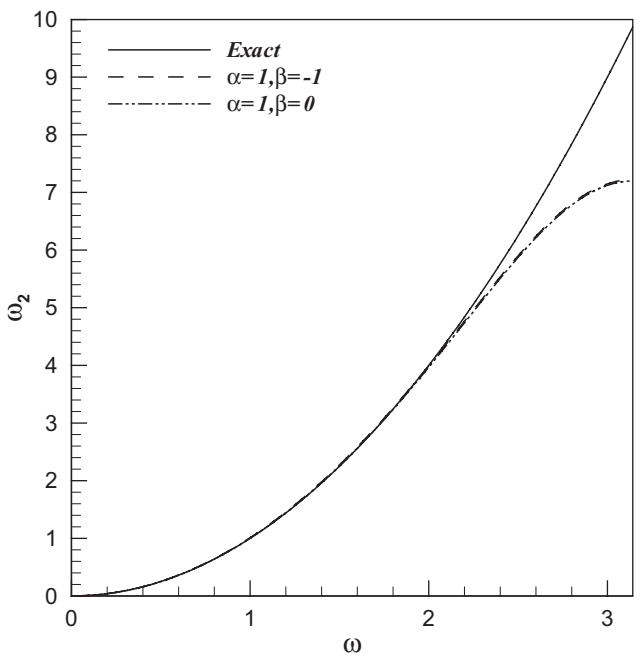

Figure 8. Comparisons of the second modified wave number for $k = 1.01$ and two different values $\alpha = 1, \beta = -1$ and $\alpha = 1, \beta = 0$.

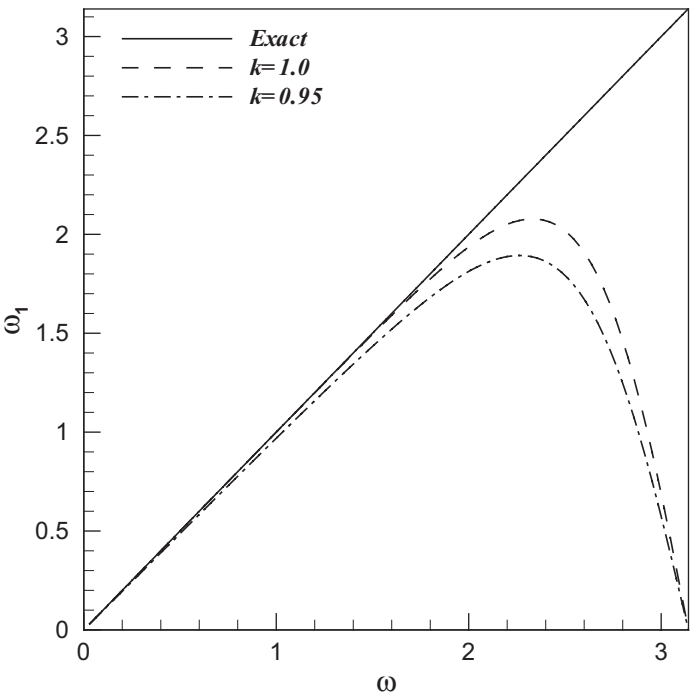

Figure 9. Comparisons of the first modified wave number for $\alpha = 1, \beta = 1$ and two different values $k = 1,\ k = 0.95$.

be obtained as,

$$\omega_1 = \frac{90\sin(\omega) - 18\sin(2\omega) + 2\sin(3\omega)}{30(1+\sigma)} \tag{13}$$

Now it is possible to compare the behaviour of the two schemes in a non-uniform grid. Figure 13 shows the plots of the modified wave number ω_1 for the uniform grid (i.e. $\sigma = 1$) and for a non-uniform grid with aspect ratio $k = 1/\sigma = 1.1$. It can be seen that the sixth-order SCFDM is more accurate than the traditional sixth-order difference method and shows better resolving property in the uniform grid. Both of the schemes are not efficient in a non-uniform grid but it seems that the sixth-order super compact method is more sensitive to the aspect ratio compared to the traditional sixth-order finite difference method for the large wave numbers.

4. THE MODIFIED EQUATION APPROACH

The results of the Fourier analysis obtained in the previous section lead to a visual representation of the error of the SCFDM in non-uniform grids. For the sake of obtaining a mathematical representation of the error and the role of the aspect ratio in the accuracy of

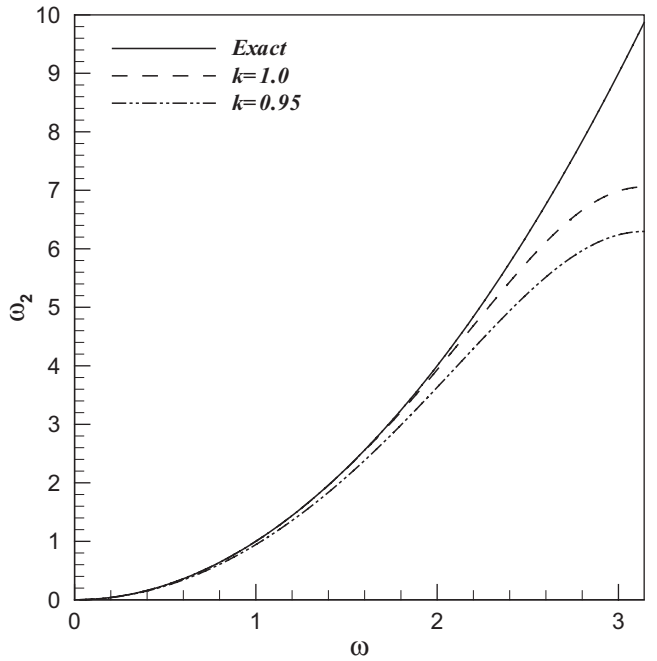

Figure 10. Comparisons of the Second modified wave number for $\alpha = 1, \beta = -1$ and two different values $k = 1, 0.95$.

the method in non-uniform grids, the modified equation approach [11, 12] is used to derive the modified equation for 1-D linear advection equation,

$$\frac{\partial u}{\partial t} + c\frac{\partial u}{\partial x} = 0 \tag{14}$$

where c is a constant. A forward temporal differencing is used to discretize the equation as below:

$$\frac{u_j^{n+1} - u_j^n}{\Delta t} + c\left(\frac{\partial u}{\partial x}\right)_j = 0 \tag{15}$$

in which n and j are the indices for time and space, respectively. To discretize the spatial derivative of the above equation using the sixth-order super compact formulation, first it is necessary to obtain an alternative form of the SCFDM relations which is introduced here for the first time. By using the forward and backward operators which were defined at the previous sections, the left-hand side of Equation (6) can be written as,

$$-\frac{1}{2}\mathbf{L}\left(\frac{1}{\sigma_j}\right)\mathbf{F}_{j-1} + (\mathbf{A} + \mathbf{L})\mathbf{F}_j - \frac{1}{2}\mathbf{L}(\sigma_{j+1})\mathbf{F}_{j+1}$$

$$= \left[\frac{1}{2}(-\mathbf{L}_2\delta^+ + \mathbf{L}_3\delta^- - \mathbf{L}_2 - \mathbf{L}_3) + \mathbf{A} + \mathbf{L}_1\right]\mathbf{F}_j$$

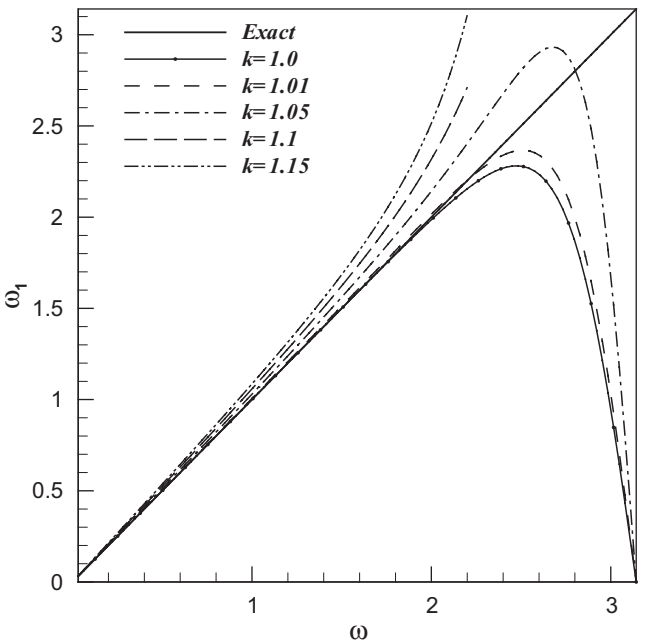

Figure 11. Comparisons of the first modified wave number for different values of k ($\alpha = 1$ and $\beta = 1$). For the eighth-order SCFDM relations.

where

$$\mathbf{L}_1 = \mathbf{L}(1), \quad \mathbf{L}_2 = \mathbf{L}(\sigma_{j+1}), \quad \mathbf{L}_3 = \mathbf{L}\left(\frac{1}{\sigma_j}\right)$$

substitution of the above equation into Equation (6) leads to the following equation:

$$[\tfrac{1}{2}(-\mathbf{L}_2\delta^+ + \mathbf{L}_3\delta^- - \mathbf{L}_2 - \mathbf{L}_3) + \mathbf{A} + \mathbf{L}_1]\mathbf{F}_j = \tfrac{1}{2}(\alpha\delta_x^+ + \beta\delta_x^-)f_j\mathbf{E} \tag{16}$$

and the approximation of the different derivatives can be obtained as follows:

$$\mathbf{F}_j = \{\mathbf{Q}^{-1}\,\tfrac{1}{2}(\alpha\delta_x^+ + \beta\delta_x^-)\}f_j\mathbf{E} \tag{17}$$

in which

$$\mathbf{Q} = [\tfrac{1}{2}(-\mathbf{L}_2\delta^+ + \mathbf{L}_3\delta^- - \mathbf{L}_2 - \mathbf{L}_3) + \mathbf{A} + \mathbf{L}_1]$$

4.1. Alternative form of the sixth-order formulation

It is assumed that $\alpha = \beta = 1$ and the variable, σ_j, is considered to be constant equal to σ. After bypassing some manipulations, the approximation of the first derivative represented by the sixth-order formulation becomes:

$$f_j^{\langle 1\rangle} = \frac{\mathbf{P}_1}{\mathbf{P}_2}\,\frac{\delta^\circ}{2}\,f_j \tag{18}$$

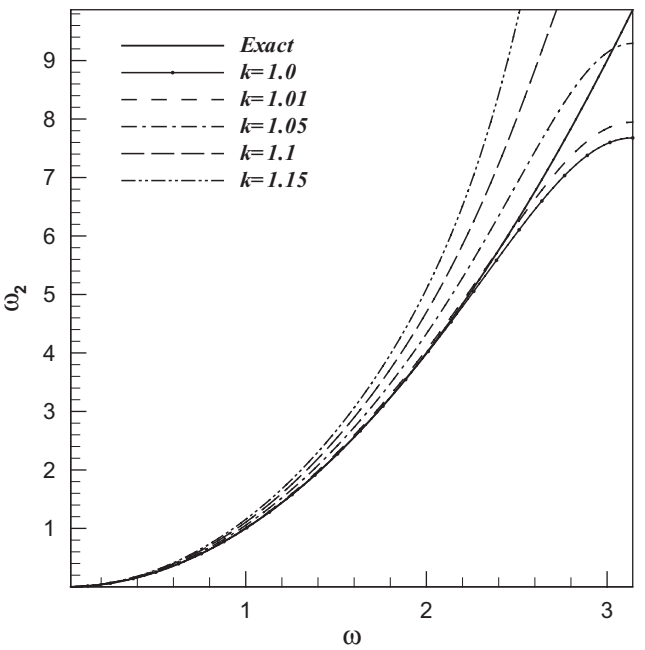

Figure 12. Comparisons of the second modified wave number for different values of k ($\alpha = 1$ and $\beta = -1$). For the eighth-order SCFDM relations.

where $\delta^{\circ} = \delta^{+} + \delta^{-}$ and the spatial operators $\mathbf{P}_1$ and $\mathbf{P}_2$ are complicate functions in the following forms:

$$\mathbf{P}_1 = \mathbf{P}_1(\sigma, \delta^{-}, \delta^{+}, \delta^{-2}, \delta^{+2}, \delta^{-3}, \delta^{+3}, \delta^{-}\delta^{+}, \delta^{-2}\delta^{+}, \delta^{-}\delta^{+2})$$

$$\mathbf{P}_2 = \mathbf{P}_2(\sigma, \delta^{-}, \delta^{+}, \delta^{-2}, \delta^{+2}, \delta^{-3}, \delta^{+3}, \delta^{-4}, \delta^{+4}, \delta^{-}\delta^{+}, \delta^{-2}\delta^{+},$$
$$\delta^{-}\delta^{+2}, \delta^{-3}\delta^{+}, \delta^{-}\delta^{+3}, \delta^{-2}\delta^{+2})$$

which are not presented here.

4.1.1. Modified equation. Equation (18) is used to discretize the spatial derivative of Equation (15)

$$\mathbf{P}_2 u_j^{n+1} - \mathbf{P}_2 u_j^{n} = v\mathbf{P}_1 \delta^{\circ} u_j^{n} \tag{19}$$

where $v = -c\Delta t/2h_j$. After the application of the operators $\mathbf{P}_1$, $\mathbf{P}_2$ and δ° and using the Taylor series and following the procedure of the derivation of the modified equation [12], the resulting modified equation will be:

$$u_t + cu_x = \xi_1(\sigma)u_x + \xi_2(\sigma)u_{xx} + \xi_3(\sigma)u_{xxx} + \xi_4(\sigma)u_{xxxx}$$
$$+\xi_5(\sigma)u_{xxxxx} + \xi_6(\sigma)u_{xxxxxx} + \xi_7(\sigma)u_{xxxxxxx} + \cdots \tag{20}$$

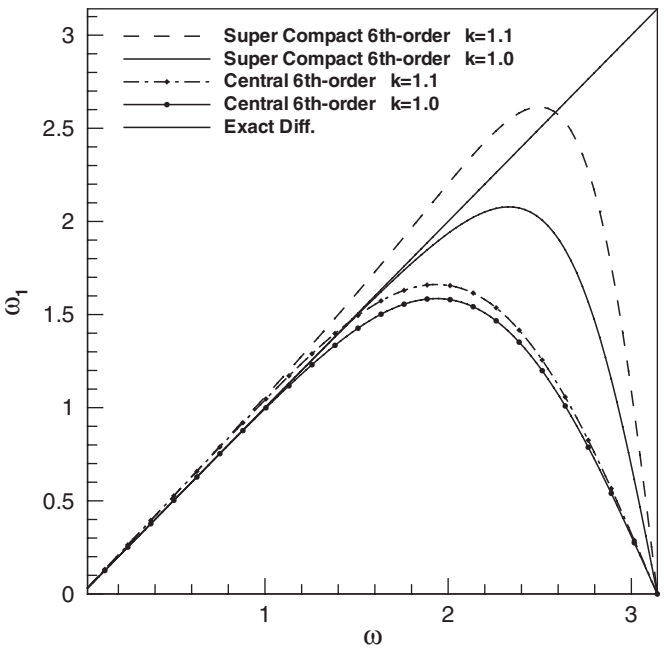

Figure 13. Comparisons of the first modified wave number for the sixth-order SCFDM and traditional sixth-order difference methods in uniform and non-uniform grids.

where the subscripts x and t denote the derivative. Coefficients ξ_1 to ξ_7 are very complicated functions of σ, h_j, h_{j-1}, c and Δt and here the simplest one i.e. ξ_1 is presented:

$$\xi_1 = -\frac{ca}{2}(\sigma + 1) + c$$

where a is a function of σ i.e. $a = a(\sigma)$. In a uniform grid where $\sigma = 1$, the functions ξ_1 to ξ_6 are independent of σ (as it can be seen for ξ_1 where $a(1) = 1$) and the method is exactly sixth-order. But in the non-uniform grid all of the coefficients ξ_1 to ξ_6 have values depending on the σ. This fact shows the dependency of the error on the aspect ratio and clarifies the crucial role of the aspect ratio in the accuracy of the SCFDM in non-uniform grids. To demonstrate the behaviour of the coefficients of the modified equation, the value of ξ_1 (for instance) at different aspect ratios is summarized at Table I. This table shows that in the non-uniform grids, when the aspect ratio is not close to one, the method is not as accurate as it was expected and even it can behave like a first-order scheme.

In the following sections, the solution of the Blasius boundary layer and non-linear parabolized stability equations (PSE) as examples which require non-uniform grid spacing are presented. The sixth-order super compact formulation in non-uniform grid is used to solve these equations and to investigate the effect of non-uniform grid on numerical accuracy.

Table I. The values of ξ_1 for different aspect ratios.

σ	Aspect ratio $k=1/\sigma$	$a(\sigma)$	$\xi_1(\sigma)/c$
1.00	1.00	1.00	0.0
0.99	1.01	1.00495	2.50×10^{-5}
0.95	1.05	1.02376	6.15×10^{-4}
0.91	1.10	1.04515	2.36×10^{-3}
0.87	1.15	1.06434	5.07×10^{-3}
0.83	1.20	1.08148	8.64×10^{-3}

5. BLASIUS BOUNDARY LAYER

In this section, the solution of the Blasius boundary layer using the sixth-order super compact formulation in a non-uniform grid spacing is presented. By defining the dimensionless similarity variables for laminar boundary layer flow over a flat plate a differential equation (the Blasius equation) is obtained [13]:

$$F''' + \tfrac{1}{2}FF'' = 0 \tag{21}$$

with boundary conditions:

$$F(0) = F'(0) = 0, \quad F'(\infty) = 1$$

where $F(\eta)$ is the Blasius function defined as:

$$\Psi = \sqrt{\nu U_\infty} x F(\eta), \quad \eta = y\sqrt{\frac{U_\infty}{\nu x}}$$

and Ψ is the stream function. We applied the sixth-order SCFDM to solve this equation for the different aspect ratios. The sixth-order SCFDM formulation for each variable has four relations, one of them is the basic equation and the others are auxiliary equations. In these set of equations there are five unknowns $\{f, f', f'', f''', f''''\}^{\mathrm{T}}$ where $(')$ denotes the derivative. The governing equation is needed to close the system and a block tridiagonal system is obtained with a block size 5×5.

Table II shows the results of numerical solution for $F''(0)$. Also a comparison is made between the results of the SCFDM and those obtained from the application of the spectral method [14]. This table also shows the number of grid points in the non-uniform grid system with $\eta_{\max} = 12$ and the number of grid points are chosen such that the grid spacing for the first grid is $h_1 = \eta_2 - \eta_1 \approx 0.01$. This choice allows us to have enough grid points in the boundary layer to obtain an accurate result. In addition, in this table the results of the SCFDM are presented for a grid distribution similar to the grid used for the spectral method.

Important role of the aspect ratio in the behaviour of the super compact scheme in non-uniform grid is illustrated by computing the error of this scheme based on spectral method. This error is shown in Table II. It can be seen that the aspect ratios which are larger than a certain limit (e.g. for sixth-order case $k = 1.2$) generate numerical errors which are not acceptable.

Table II. Comparison of the results of the sixth-order SCFDM for the Blasius equation for the different aspect ratios in a non-uniform grid.

Method	$F''(0)$	Number of grids	Error (%)
SCFDM $k=1.00$	0.332057	1201	~ 0
SCFDM $k=1.01$	0.332057	250	~ 0
SCFDM $k=1.05$	0.332057	85	~ 0
SCFDM $k=1.10$	0.332057	51	~ 0
SCFDM $k=1.15$	0.332056	37	3×10^{-4}
SCFDM $k=1.20$	0.332054	31	9×10^{-4}
SCFDM $k=1.50$	0.331696	16	0.1
SCFDM (spectral grid)	0.332057	76	—
Spectral method	0.332057	31	—

6. PARABOLIZED STABILITY EQUATIONS

The PSE are an initial-boundary value problem and they can be solved using a marching procedure. As a result, the computational effort and required storage can be reduced using the PSE. Therefore, these equations are appropriate for a rapid and an accurate prediction of laminar-turbulent transition of incompressible boundary layers (more details are given in Reference [15]).

6.1. Problem formulation

In this subsection, the stability of incompressible flow over a flat plate in Cartesian co-ordinate system is formulated. The Cartesian co-ordinates are denoted by x, y, and z, where x is the streamwise distance from the leading edge, and y and z are the plate normal and the spanwise co-ordinates, respectively. All quantities are non-dimensionalized with the free stream velocity U_∞ and the fixed length $\delta_\circ = \delta(x_\circ) = \sqrt{\nu x_\circ / U_\infty}$, where $x_\circ$ is a fixed starting dimensional distance from the leading edge and ν is kinematic viscosity. The resulting non-dimensional parameter is the reference Reynolds number $R_\circ = U_\infty \delta_\circ / \nu$ at $x = x_\circ$. Then, the three dimensional incompressible Navier–Stokes equations in non-dimensional form are as follows:

$$\nabla \cdot V = 0 \tag{22}$$

$$\frac{\partial V}{\partial t} + (V \cdot \nabla)V = -\nabla p + \frac{1}{R_\circ}\nabla^2 V \tag{23}$$

where $V = (u, v, w)$ is the velocity vector and p is the pressure.

To obtain the disturbance equations, one can split the dependent quantities vector $\phi = (u, v, w, p)^{\mathrm{T}}$ into a steady two-dimensional mean value (basic flow) $\Phi_b = (U_b, V_b, 0, P_b)^{\mathrm{T}}$ and an unsteady three-dimensional perturbation quantity $\phi' = (u', v', w', p')^{\mathrm{T}}$ i.e.

$$\phi(x, y, z, t) = \Phi_b(x, y) + \phi'(x, y, z, t) \tag{24}$$

By substituting the vector ϕ into the Navier–Stokes equations (22) and (23), and subtracting the terms satisfied by the basic flow, one will obtain the governing equations for the disturbances ϕ', which will not be presented here.

For flow over the flat plate the basic flow can be obtained by solving the self-similar boundary layer equations (the Blasius equation).

6.2. Non-linear PSE

For non-linear waves, the total disturbance is assumed to be periodic in time and in the spanwise direction. For most problems, it is sufficient to choose a finite number of modes. In these cases, the total disturbance vector $\phi'(x, y, z, t)$ can be expressed as follows:

$$\phi' = \sum_{n=-N}^{N} \sum_{m=-K}^{K} \hat{\phi}_{nm}(x, y)\chi_{nm}(x, z, t) \tag{25}$$

where the shape function vector $\hat{\phi}_{nm}$ and χ_{nm} are:

$$\hat{\phi}_{nm} = (\hat{u}_{nm}, \hat{v}_{nm}, \hat{w}_{nm}, \hat{p}_{nm})^{\mathrm{T}}$$

$$\chi_{nm} = \exp\left[\mathrm{i}\left(\int_{x_\circ}^{x} \alpha_{nm}(s)\,\mathrm{d}s + m\tilde{\beta}z - n\tilde{\omega}t\right)\right]$$

The non-linear PSE are obtained by substituting the disturbance vector ϕ' into the non-linear disturbance equations and performing harmonic balance for both linear and non-linear terms. Finally, the non-linear PSE equations can be obtained for the shape function $\hat{\phi}_{nm}$ of a single Fourier mode (n, m), that can be written as a system of differential equations in terms of stability variables $\hat{\mathbf{q}}_{nm}$ as follows:

$$\mathbf{L}(\alpha_{nm})[\hat{\mathbf{q}}_{nm}] + \mathbf{M}(\alpha_{nm})\left[\frac{\partial \hat{\mathbf{q}}_{nm}}{\partial x}\right] = H_{nm} \tag{26}$$

where

$$\hat{\mathbf{q}} = (\hat{u}, \hat{v}, \hat{w}, \hat{p})^{\mathrm{T}}$$

and H_{nm} is non-linear forcing function.

The PSE equations need appropriate boundary conditions in the y direction. At the wall, the components of the perturbation velocity satisfy the no-slip condition

$$\hat{u} = \hat{v} = \hat{w} = 0, \quad y = 0 \tag{27}$$

and the Dirichlet conditions are applied in the free-stream,

$$\hat{u} = \hat{v} = \hat{w} = 0, \quad y \to \infty \tag{28}$$

6.3. Numerical solution

The sixth-order SCFDM formulation for non-uniform grid points is used to compute the basic flow and the PSE equations. Numerical solution of PSE equations needs to discretize equation (26) in both streamwise (x) and wall normal (y) directions. In the streamwise direction, the

first-order backward difference schemes is used. In the wall normal direction, the sixth-order SCFDM is employed. By using the sixth-order SCFDM formulation in y direction for each unknown, 20 equations are obtained (16 relations for SCFDM and four relations are governing equations).

These equations require 20 boundary conditions. Equations (27) and (28) provide six boundary conditions. An additional boundary condition is obtained using the derivative of continuity equation at the wall. Other boundary conditions are obtained as a part of solution, by using forward and backward SCFDM relations at boundaries. The above system of equations along with the 20 boundary conditions give a block tridiagonal system of equations with a block size of 20×20.

6.4. Initial conditions

The initial conditions for the PSE computation are obtained by solving the Orr–Sommerfeld equations at the corresponding Reynolds number $R_\circ$ and non-dimensional frequency F ($\omega\nu/U_\infty^2\times10^6$). The Orr–Sommerfeld equations in primitive forms can be obtained from the linear PSE equations by setting $\partial/\partial x$ derivatives and V_b equal to zero and can also be solved using the super compact method.

6.5. Results and discussion

All calculations initiated at $R_\circ = 400$ where the shape function and corresponding wave number for the TS wave are provided by the Orr–Sommerfeld solutions.

6.5.1. 3-D non-linear PSE. There are different routes to transition depending on the initial conditions. The most dangerous route is expected to be a three-dimensional subharmonic mode interaction. A non-linear interaction is considered between a TS fundamental wave (mode $(2,0)$) $2F = 124$ and a pair of subharmonic oblique waves ($(1,1)$ and $(1,-1)$ modes) for conditions of Kachanov and Levchenko's [16] experiment. The initial amplitudes of the TS wave and the subharmonic wave are chosen $A^\circ_{2,0} = 0.46\%$ and $A^\circ_{1,1} = 0.01\%$ based on $u'_{\max}$, respectively. The spanwise wave number of the subharmonic mode is fixed at $\tilde{\beta} = 0.14$. The stepsize for the marching procedure is $\Delta x = 15$. The solution is obtained with Fourier series truncated to $N = 2$, and $K = 1$, and extended from $Re = 400$ to $Re = 720$. Figure 14 shows the PSE results for the amplitudes of three modes $(0,0)$, $(1,1)$ and $(2,0)$ based on $u'_{\max}$ together with experimental data for H-type breakdown. Amplitudes were measured at $\eta = 1.3$. This figure indicates that the results of the SCFDM agree well with those of the fourth-order compact [17] (not shown here) and experimental data, when $k = 1.01$ is used. For $k = 1.15$, a numerical error is generated from the first steps of computation as shown in the figure. Because of these errors the code dose not converge at $Re = 680$ and breaks down. The velocity profiles of u' for mode $(1,1)$ at $Re = 608$ for $A^0_{1,1} = 0.01\%$ is shown in Figure 15. When $k = 1.01$, results show better agreement with experimental data and DNS results computed by Fasel *et al.* [18]. The differences between the PSE and the experimental results for this mode (subharmonic) may come from the initial conditions which are provided by the Orr–Sommerfeld equations. Figure 16 presents the variations of non-dimensional skin friction coefficient versus Reynolds number for the subharmonic breakdown. The figure also shows the comparison of the results with those obtained by the fourth-order compact method [17] to indicate the accuracy of the computation. As it can be seen for $k = 1.15$ used in the

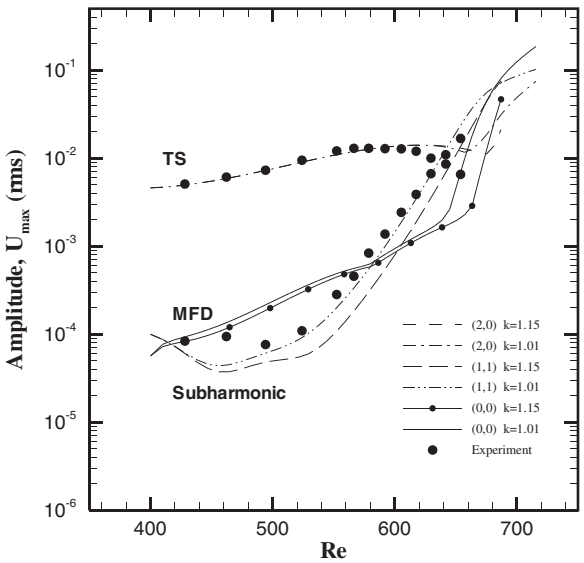

Figure 14. Comparison of amplitudes based on $u'_{\max}$ versus Reynolds number for subharmonic breakdown, for two different non-uniform grid $k = 1.01$ and 1.15. Dots denote experimental data.

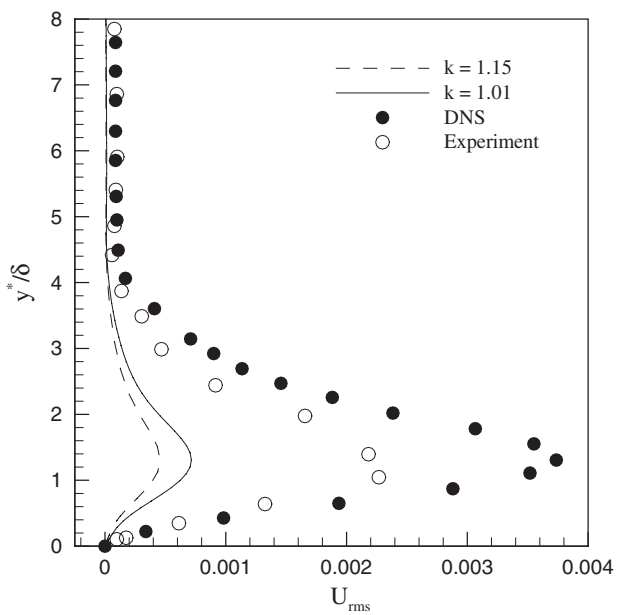

Figure 15. Comparison of velocity profiles of u' for various modes at $Re = 608$ and $2F = 124$, for two cases $k = 1.01$ and 1.15. Circles denote DNS results by Fasel *et al.* [18] and dots are experimental data.

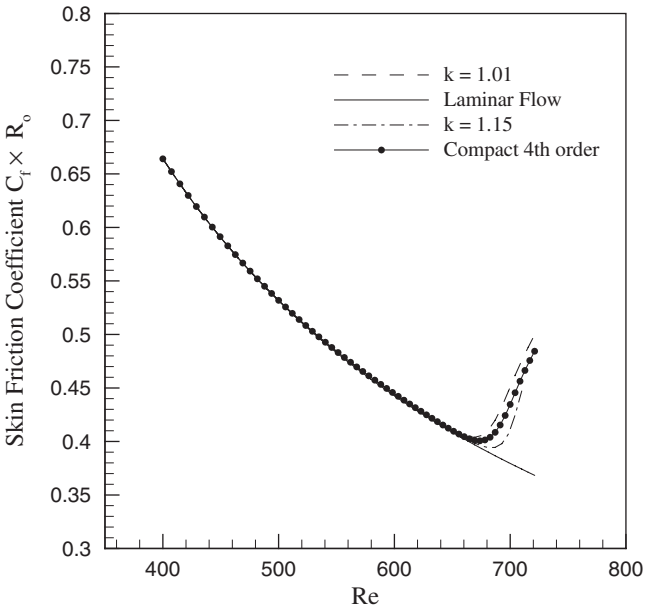

Figure 16. Comparison of non-dimensional skin friction coefficient versus Reynolds number. For cases $k = 1.01$ and 1.15, dots denote fourth-order compact method results by Esfahanian *et al.* [17].

SCFDM, the numerical errors initiated from the first steps of computation, affect the rise of the skin friction coefficient.

7. CONCLUSIONS

The accuracy of the super compact finite difference method (SCFDM) in non-uniform grid points has been studied. The Fourier analysis and the modified equation approach are used to investigate the accuracy. The Fourier analysis gives a visual representation of the error of the SCFDM in non-uniform grid introduced at different aspect ratios respect to the uniform grid. Further, the modified equation approach leads to a mathematical representation of the error and clarifies the role of the aspect ratio in the accuracy. These results show that by choosing the aspect ratio close to one, the accuracy of the SCFDM is almost like uniform grid. The sixth-order super compact relations in non-uniform grid are used to solve the Blasius equation. The results show that different aspect ratios up to a certain limit are acceptable to have an accurate solution. In addition, the sixth-order super compact relations in the non-uniform grid are applied to solve parabolized stability equations (PSE) which are more sensitive to numerical accuracy. For the PSE equations it was found that there are more limitation to the aspect ratio than the case of Blasius equation for accurate solution and the aspect ratio must be chosen very close to one.

ACKNOWLEDGEMENTS

Authors would like to thank University of Tehran and Atmospheric Science & Meteorological Research Center (ASMERC) of Iran for financial support of this research.

REFERENCES

1. Numerov BV. A method of extrapolation of perturbations. *Monthly Notices of the Royal Astronomical Society* 1924; **84**:592–601.
2. Fox L, Goodwin ET. Some new methods for the numerical integration of ordinary differential equations. *Proceedings of the Cambridge Philosophical Society for Mathematics and Physics* 1949; **45**:373–388.
3. Kreiss HO, Oliger J. Comparison of accurate methods for the integration of hyperbolic equations. *Tellus* 1972; **24**:199–215.
4. Hirsh SR. Higher order accurate difference solutions of fluid mechanics problems by a compact differencing technique. *Journal of Computational Physics* 1975; **19**:90–109.
5. Lele SK. Compact finite difference schemes with spectral-like resolution. *Journal of Computational Physics* 1992; **103**:16–42.
6. Dexun Fu, Yanwen Ma. High resolution schemes. In *Computational Fluid Dynamics Review*, Hafez M, Oshima K (eds). Wiley: New York, 1995.
7. Yanwen Ma, Dexun Fu. Super compact finite difference method with uniform and non-uniform grid system. *Proceedings of 6th International Symposium on Computational Fluid Dynamics*, vol. 3, Lake Tahoe, Nevada, 1995.
8. Yanwen Ma, Dexun Fu. Super compact finite difference method (SCFDM) with arbitrary high accuracy. *Computational Fluid Dynamics Journal* 1996; **5**(2):259–276.
9. Dexun Fu, Yanwen Ma. Analysis of super compact finite difference method and application for simulation of vortex–shock interaction. *International Journal for Numerical Methods in Fluids* 2001; **36**:773–805.
10. Vichnevetsky R, Bowles JB. *Fourier Analysis of Numerical Approximations of Hyperbolic Equations*. SIAM: Philadelphia, 1982.
11. Warming RF, Hyet BJ. The modified equation approach to the stability and accuracy analysis of finite difference methods. *Journal of the Computational Physics* 1974; **14**:159–179.
12. Tannehil JC, Anderson DA, Pletcher RH. *Computational Fluid Mechanics and Heat Transfer* (2nd edn). Taylor & Francis: Bristol, PA, 1997.
13. White FM. *Viscous Fluid Flow*. McGraw-Hill: New York, 1991.
14. Esfahanian V. Computational and stability analysis of laminar flow over a blunted cone in hypersonic flow. *Ph.D. Thesis*, The Ohio State University, Columbus, OH, 1991.
15. Bertolotti FP. Linear and nonlinear stability of the boundary layers with streamwise varying properties. *Ph.D. Thesis*, The Ohio State University, Columbus, OH, 1991.
16. Kachanov YS, Levchenko VY. The resonant interaction of disturbances at laminar-turbulent transition in a boundary layer. *Journal of Fluid Mechanics* 1984; **138**:209–247.
17. Esfahanian V, Hejranfar K, Sabetghadam F. Linear and non-linear PSE for stability analysis of the Blasius boundary layer using compact scheme. *Journal of Fluids Engineering* (ASME) 2001; **123**(3):545–550.
18. Fasel HF, Rist U, Konzelmann U. Numerical investigation of the three-dimensional development in boundary-layer transition. *AIAA Journal* 1990; **28**(1):29–37.

